Supplementary Materials: A New Temperature-Vegetation Triangle Algorithm with Variable Edges (TAVE) for Satellite-Based Actual Evapotranspiration Estimation

Hua Zhang, Steven M. Gorelick, Nicolas Avisse, Amaury Tilmant, Deepthi Rajsekhar, and Jim Yoon

Table S1. Summary of studies that addressed the terrain effects in temperature-vegetation triangle methods.

Method	Imagery	Study area	Elevation (m)	Area (km²)
T_a correction using DEM and a standard lapse rate and Ts correction using terrain slope and aspect and satellite view path [1]	MODIS	Taihu Basin, China	0–1500	36,500
T_s correction as surface potential temperature [2]	MODIS	Atlantic provinces Canada	0–834	133,852
T_a correction based on lapse rates [3]	MODIS	North-western Iran	300–3000	Unknown (35°–37°N, 47°–49°E)
T_s correction based on both standard and fitted lapse rates [4]	MODIS	Calabria, Italy	Unknown	Unknown
Removing pixels based on slope and elevation difference from the site [5]	Landsat5-TM, Envisat-AATSR/MERIS, MSG-SEVIRI	Henares River Basin, Spain	550–1500	4,136
T_a correction based on a lapse rate [6]	MODIS	Walnut Gulch Experimental Watershed, USA	1226–1929	148
Removing pixels based on average elevation [7]	MODIS	Heihe Basin, China	1200–3000	38,000

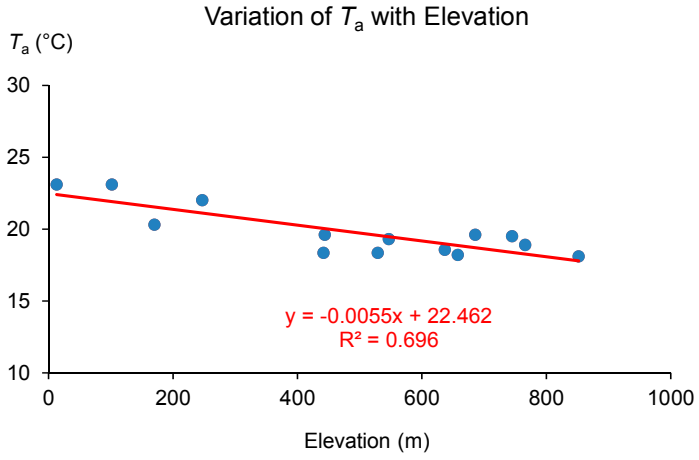

Figure S1. The relationship between annual average air temperature and elevation based on 14 ground weather stations.

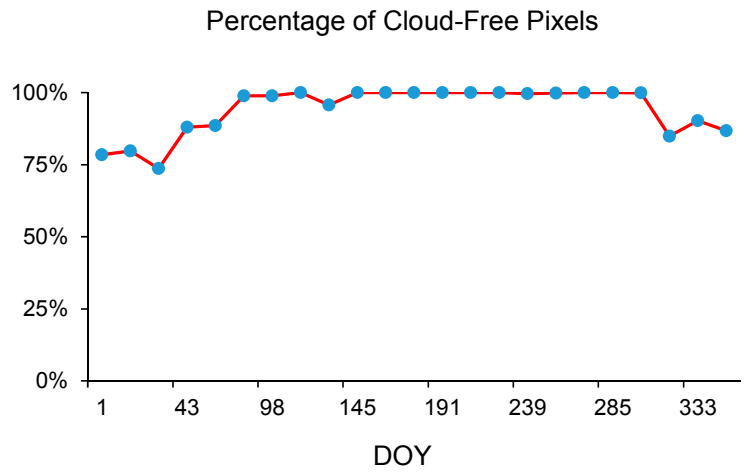

Figure S2. The percentage of cloud-free pixels in T_s images over the study domain in 2009.

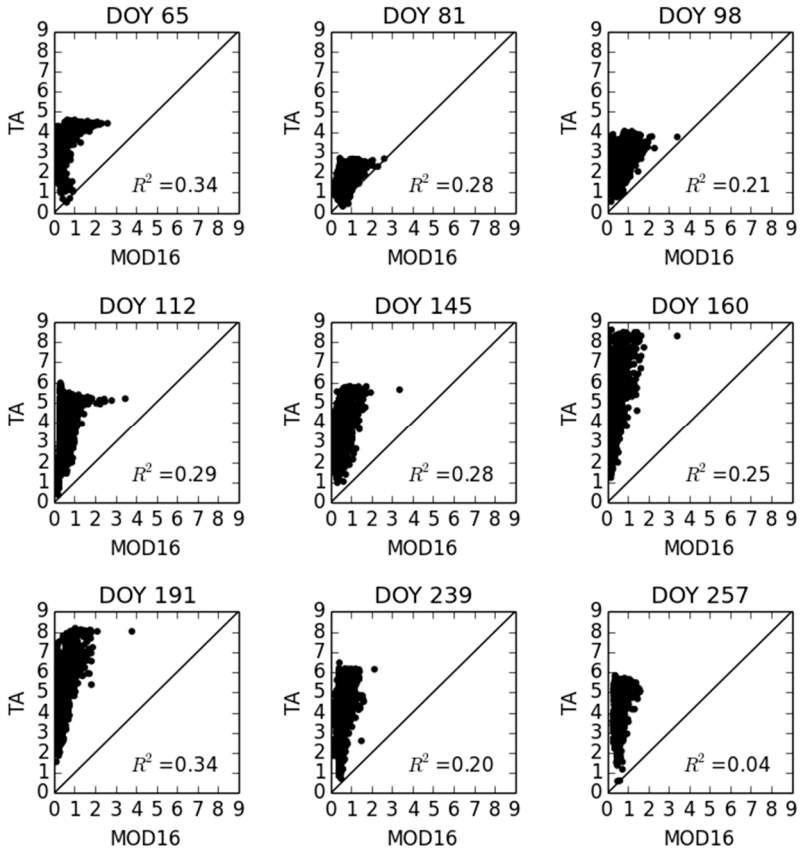

Figure S3. Comparison of the AET estimates derived by the traditional triangle method (TA) and the MODIS 16 evapotranspiration product (MOD16) over the study area on nine selected days of year (DOY). AET is in mm/day. DOY 65 and 81 are representative days of the wet season from October to March. DOY 98, 112, 145, 160, 191, 239, and 257 are representative days of the dry season from April to September. The line shown is the 1:1 line of perfect agreement between MOD16 and TAVE. The R^2 reported is for a line not shown that goes through the points shown.

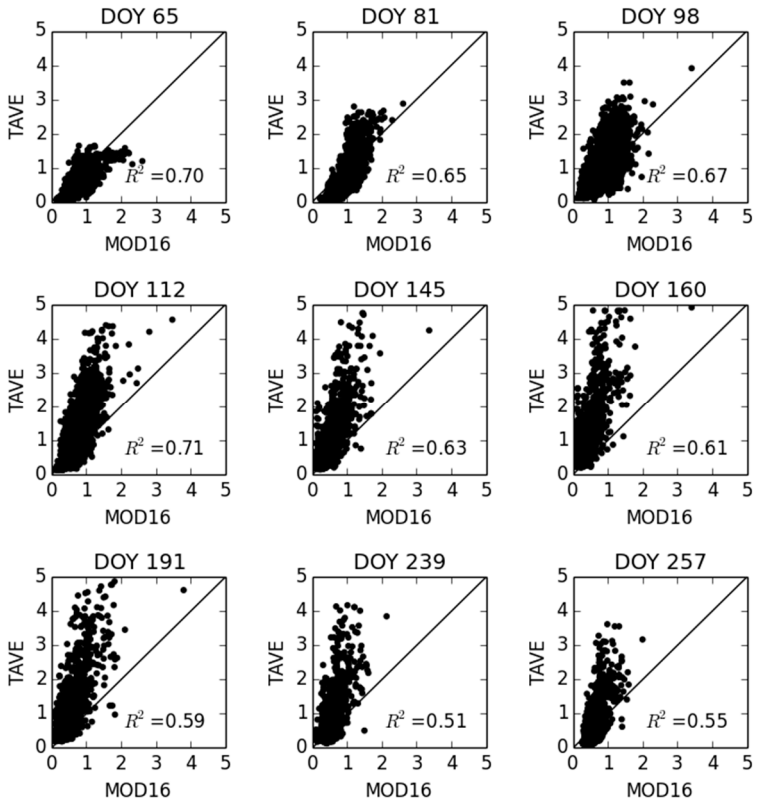

Figure S4. Comparison of the PET estimates derived by the triangle method with variable edges (TAVE), the MODIS 16 evapotranspiration product (MOD16), and pan evaporation across the study area on nine selected days of year (DOY).

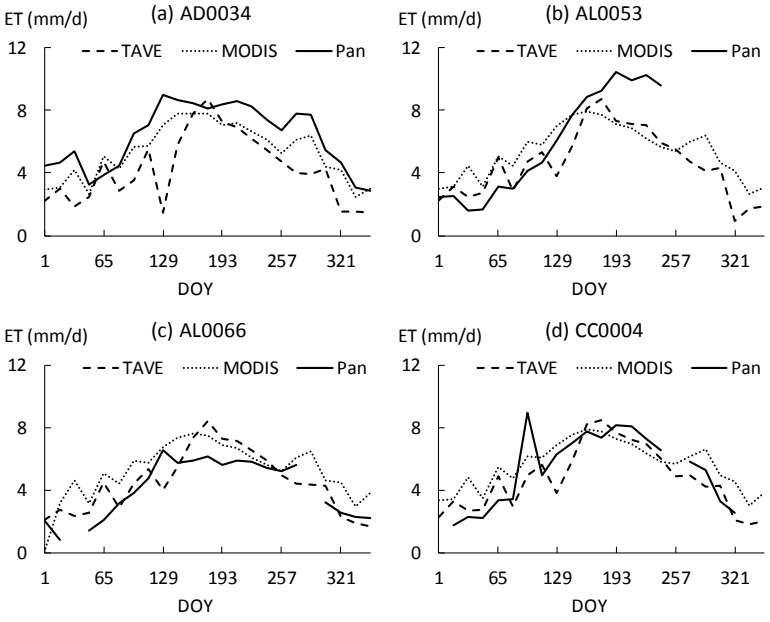

Figure S5. Comparison of satellite-derived potential evapotranspiration (PET) estimates with pan evaporation observations at four stations. Pan evaporation data using a pan coefficient of 0.7 are the average of daily records over the eight-day period of MODIS images. The empty intervals of pan evaporation data indicate missing records. The values of MODIS PET are daily rates calculated by dividing the original 8-day cumulative PET values by 8 days. AET/Pan correspond to lines shown and NDVI correspond to the upper bar graphs. The locations of the stations are indicated in Figure 1.

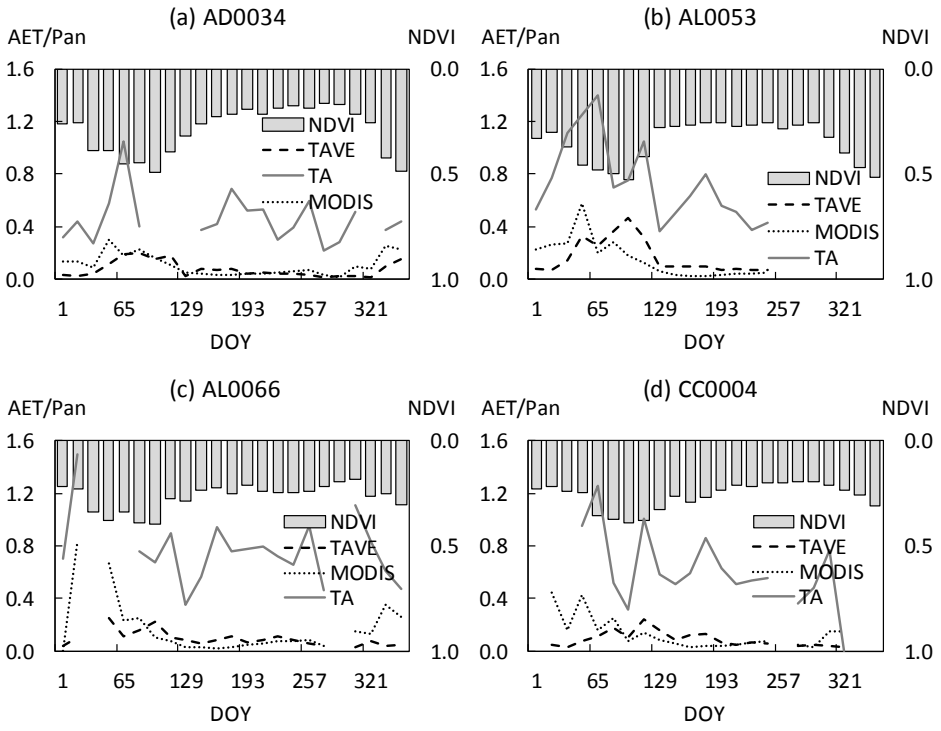

Figure S6. Comparison of satellite-derived AET estimates with pan evaporation observations at four stations. AET/Pan correspond to lines shown and NDVI correspond to the upper bar graphs. The empty intervals indicate that no AET estimates can be generated for the selected pixel because its NDVI value is below the threshold for vegetated surface.

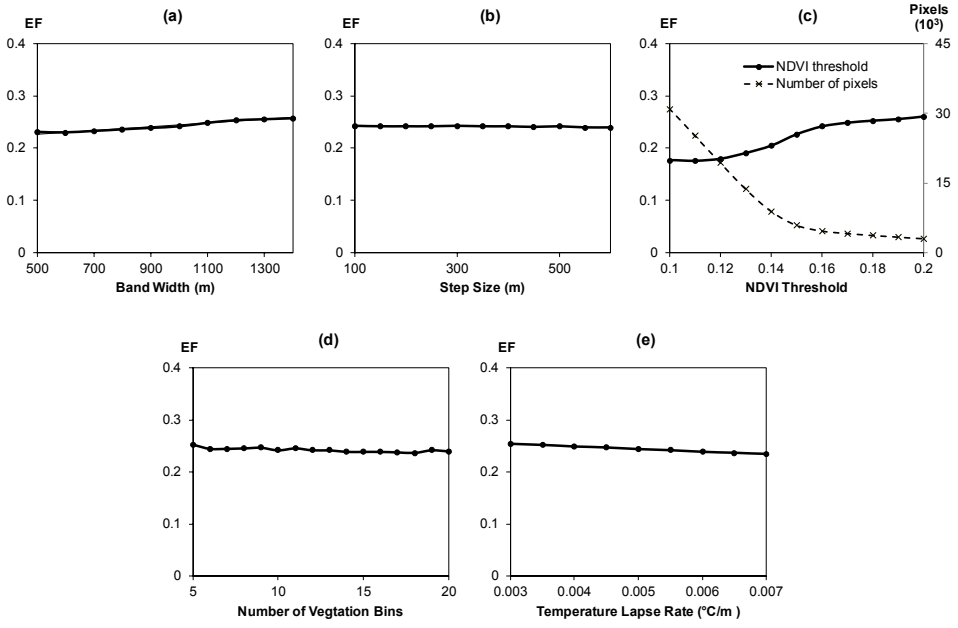

Figure S7. Sensitivity of AET estimates to TAVE parameters: (**a**) width of elevation zones, (**b**) step size of elevation zones, (**c**) number of vegetation bins, (**d**) NDVI threshold, and (**e**) temperature lapse rate. Results are based on images of June 9th (DOY 160), 2009.

References

1. Zhao, X.; Liu, Y. Relative contribution of the topographic influence on the triangle approach for evapotranspiration estimation over mountainous areas. *Adv. Meteorol.* **2014**, *2014*, 1–16.

2. Hassan, Q.; Bourque, C.; Meng, F.-R.; Cox, R. A wetness index using terrain-corrected surface temperature and normalized difference vegetation index derived from standard modis products: An evaluation of its use in a humid forest-dominated region of eastern canada. *Sensors* **2007**, *7*, 2028–2048.
3. Rahimzadeh-Bajgiran, P.; Omasa, K.; Shimizu, Y. Comparative evaluation of the vegetation dryness index (vdi), the temperature vegetation dryness index (tvdi) and the improved tvdi (itvdi) for water stress detection in semi-arid regions of iran. *ISPRS J. Photogramm. Remote Sens.* **2012**, *68*, 1–12.
4. Van Doninck, J.; Peters, J.; De Baets, B.; De Clercq, E.M.; Ducheyne, E.; Verhoest, N.E.C. Influence of topographic normalization on the vegetation index-surface temperature relationship. *J. Appl. Remote Sens.* **2012**, doi:10.1117/1.JRS.6.063518.
5. de Tomás, A.; Nieto, H.; Guzinski, R.; Salas, J.; Sandholt, I.; Berliner, P. Validation and scale dependencies of the triangle method for the evaporative fraction estimation over heterogeneous areas. *Remote Sens. Environ.* **2014**, *152*, 493–511.
6. Wang, W.; Huang, D.; Wang, X.G.; Liu, Y.R.; Zhou, F. Estimation of soil moisture using trapezoidal relationship between remotely sensed land surface temperature and vegetation index. *Hydrol. Earth Syst. Sci.* **2011**, *15*, 1699–1712.
7. Tang, R.; Li, Z.L.; Tang, B. An application of the ts–vi triangle method with enhanced edges determination for evapotranspiration estimation from modis data in arid and semi-arid regions: Implementation and validation. *Remote Sens. Environ.* **2010**, *114*, 540–551.